

LETTER TO THE EDITOR

## What is the length of a knot in a polymer ?

**B. Marcone, E. Orlandini, A. L. Stella and F. Zonta**

INFN-Dipartimento di Fisica and Sezione INFN, Università di Padova, I-35131  
Padova, Italy.

E-mail: orlandini@pd.infn.it

**Abstract.** We give statistical definitions of the length,  $l$ , of a loose prime knot tied into a long, fluctuating ring macromolecule. Monte Carlo results for the equilibrium, good solvent regime show that  $\langle l \rangle \sim N^t$ , where  $N$  is the ring length and  $t \simeq 0.75$  is independent of the knot type. In the collapsed regime below the theta temperature, length determinations based on the entropic competition of different knots within the same ring show knot delocalization ( $t \simeq 1$ ).

Submitted to: *J. Phys. A: Math. Gen.*

PACS numbers: 02.10.Kn, 36.20.Ey, 05.70.Jk, 82.35.Lr, 87.15.Aa

Long polymers are remarkable systems in which topological entanglement is almost unavoidable [1, 2] and shows consequences pertaining to many different scientific contexts. In chemistry the synthesis of macromolecules with nontrivial topology, like catenanes, is well established [3]. The role of knots and links in the biology of DNA and the existence of enzymes like topoisomerases, which control these entanglements, have been at the basis of an explosion of interest in topology among biologists, chemists, mathematicians, and physicists since the eighties [4, 5]. Most recently, techniques for manipulating single molecules opened new possibilities of knot creation and study [6, 7].

In all these examples the knowledge of the degree of localization of the knots within the chains is of primary importance. The action of topoisomerases [5, 4] certainly depends on how localized the topological entanglement is [8]. The folding dynamics of a knotted protein [9] should also be strongly influenced by the tightness of the knot. When a knot diffuses along a DNA molecule stretched by molecular tweezers, the length of the entangled region is also essential since it determines the diffusion coefficient. If the knot is tight enough this length can be approximated by that of the knot in its ideal form [7]. An ideal knot is realized with the shortest piece of rope of constant diameter and is the only one for which a precise definition of length exists [10, 11, 12]. Of course, this model is inadequate if the molecule is not well stretched and the knotted region fluctuates substantially.

In spite of several indications that prime knots of polymers in good solvent are rather well localized [13, 14], proofs and direct quantitative descriptions of this localization are still missing. This is primarily due to difficulties related to the notion of a knotted open string [15]. Indeed, to localize the knot requires to identify an open portion of the ring which is “knotted”. However, to assert that an open piece of a closed rope “contains” a knot, is ambiguous. Mathematically there are no knots in an open string since continuous deformations can always bring it into an untangled shape. Substantial progress in the description of localization properties of topological entanglement has been made for flat knots [16]. These models describe three-dimensional knotted polymers fully adsorbed on a plane with the simplifying feature that the number of overlaps is restricted to the minimum compatible with the topology. In this way knot length can be defined and studied both numerically and analytically [17]. It was also discovered that flat knots become delocalized when the adsorbed polymer undergoes theta collapse [18, 19]. A demonstration of the conjectured [18] analogous delocalization phenomenon for compact knotted polymers in three dimensions remains an open challenge [20].

In this Letter we propose a statistical description of the length,  $l$ , of a knot within a circular fluctuating polymers with  $N$  monomers. We find that  $\langle l \rangle \sim N^t$  with  $t \simeq 0.75$  in the good solvent regime (weak localization), and  $t \simeq 1$  (delocalization) in the collapsed phase [21].

We consider knotted self-avoiding polygons (SAP) on cubic lattice, which are a good model for long polymers in a good solvent [21]. If necessary, a theta collapse [21] into compact configurations can be induced by switching on an attractive interaction between

nearest neighbor lattice sites visited not consecutively by the SAP [18] and by lowering enough the temperature  $T$ .  $N$  is the number of lattice edges occupied by the SAP. A BFACF Monte Carlo dynamics [22] preserving the topology of the SAP [23] enabled the sampling of equilibrium configurations of chains of variable  $N$ . To increase mobility a multiple Markov chains [25] in the space of the edge fugacity was implemented.

A first strategy of knot length determination is as follows. In each sampled configuration, various open portions of the SAP are considered and for each one of them a closure is made by joining its ends, A and B, with an off-lattice path (Fig.1). This path is chosen in order to minimize the risk of knot modifications or disentanglements in the resulting new ring. This risk can not be fully avoided and is a possible source of systematic errors. Once the new ring has been constructed, the computation of a topological invariant, namely the Alexander polynomial [26]  $\Delta(z)$  at  $z = -1$ , allows to verify the presence and the type of knot [27]. The length  $l$  of the knot in a given SAP configuration can then be identified with the shortest ring portion still displaying the original knot, among a large set obtained by several cutting and closing operations [28]. The plot of the average length of a trefoil knot ( $3_1$ ) [26] as a function of  $N$  (Fig.2) shows full consistency with the scaling law

$$\langle l \rangle \sim N^t \quad (1)$$

with  $t = 0.74 \pm 0.14$  which is also robust with respect to a change of prime knot type. For

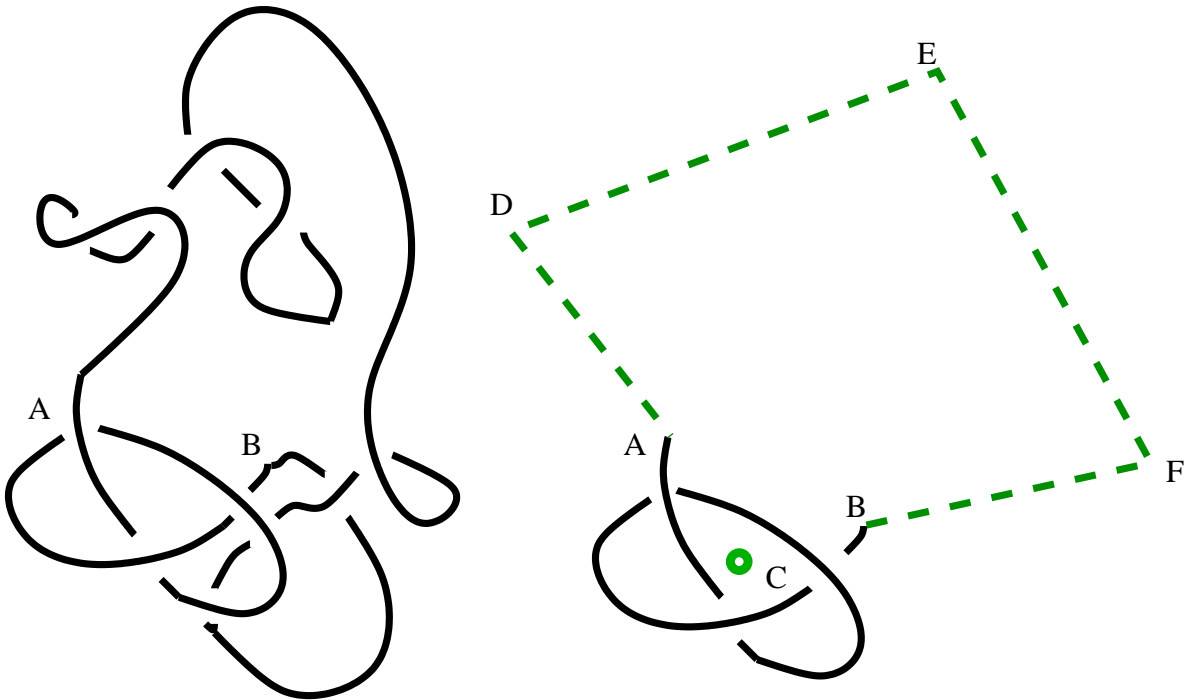


**Figure 1.** Once extracted the open string portion (AB) from the SAP, we determine its center of mass C. An off-lattice planar 4-edges polygon is attached to the extrema A and B. The polygon lies on the plane CAB. D,E and F are all chosen far away from C in order to avoid additional entanglement with the open string.

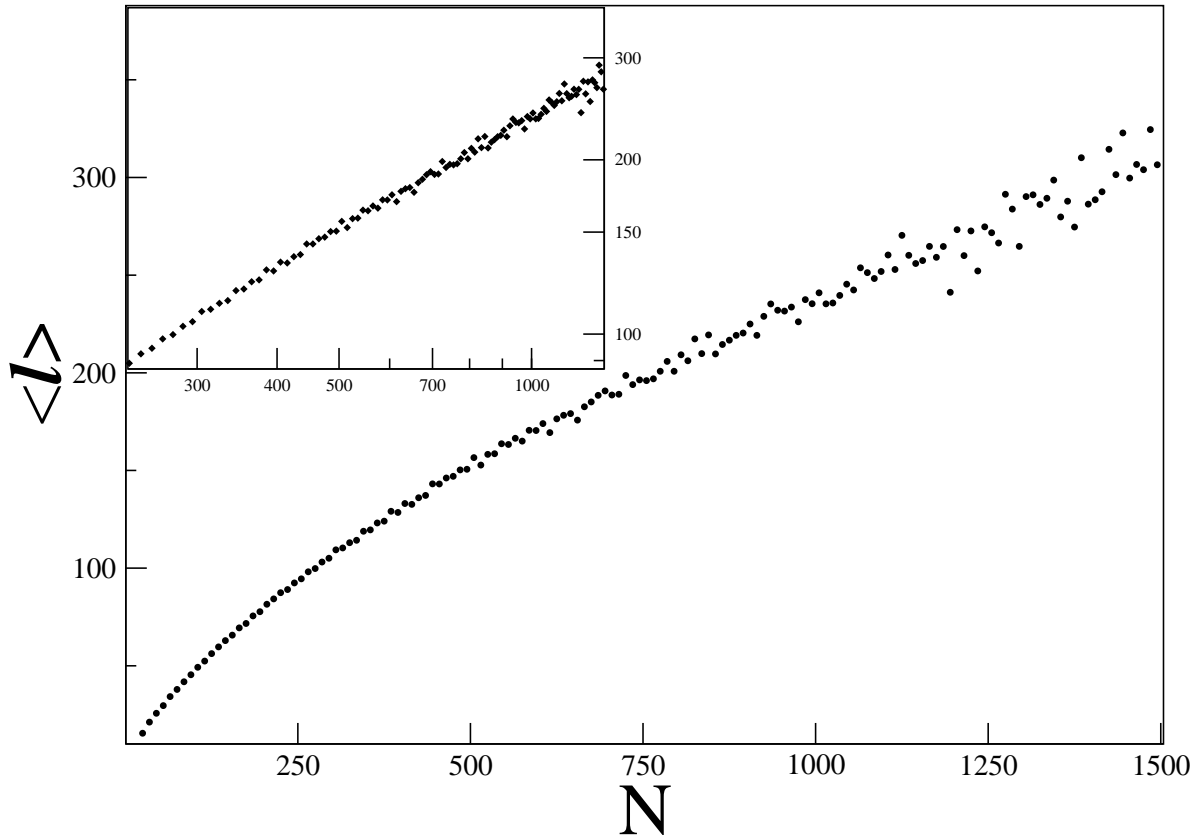


**Figure 2.**  $\langle l \rangle$  of the trefoil ( $3_1$ ) knot as a function of  $N$ . The configurations sampled were  $\sim 10^6$  in total. The brackets  $\langle \cdot \rangle$  denote averages taken over data binned around fixed values of  $N$ . The inset shows the log-log version of the plot.

example, if we replace the  $3_1$  by a  $4_1$  or  $5_1$  knot [26], Eq.(1) remains valid with the same  $t$  within confidence limits. Unfortunately, one can not estimate the possible systematic errors arising from the cutting and closing procedure used in this analysis [29], which would be a serious handicap for applications to compact polymers. Thus, one needs to validate the law in Eq.(1) by alternative, consistent methods of length determination.

Consider a SAP partitioned into two loops by a narrow slip link. Each loop is tied into a  $3_1$  knot and the Monte Carlo dynamics is such that each knot cannot translocate from its loop to the other one (Fig. 3). The two loops also remain unlinked. Since the number of configurations for the whole ring is maximum when one of the loops is much longer than the other one, most configurations break the symmetry between the two loops showing a marked length unbalance. Typically, in one of the two loops the knot has a very large share of the whole ring at its disposal, while the other loop is just long enough to host its knot. Consequently, we choose to always identify the length of the shorter loop with the length,  $l$ , of a trefoil knot inserted in a SAP. Such  $l$  is always sampled now in situations in which the two ends of the knot come close to each other in the neighborhood of the slip link. However, one can hope this statistic to be representative of more general samples if laws like Eq.(1) are considered. Indeed,

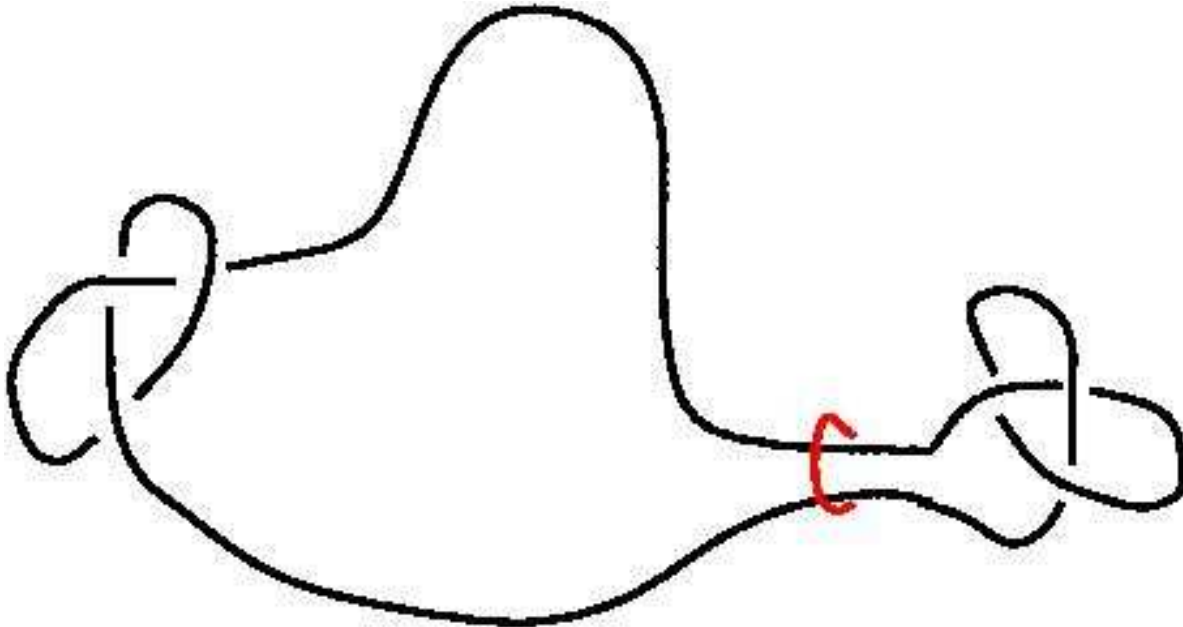


**Figure 3.** Sketch of a  $3_1$  knot (right) forced to its typical length by the entropic competition between knotted loops. To simulate the slip link we impose the constraint that two fixed parallel edges of the polygon have always to be kept one lattice distance apart [28].

for the average of this  $l$  the power law behaviour reported in Eq.(1) still holds, with  $t = 0.74 \pm 0.05$ , consistent with the previous estimate (Fig. 4). In the case of two unknotted loops we verified that the average length of the shorter one does not grow appreciably with  $N$ , further supporting our interpretation of  $l$  as the knot length in the  $3_1$  vs  $3_1$  case.

This last method of length determination needs a suitable competition between the two loops [30]. If only one of them were left unknotted, a too strong dominance of the knotted loop would result, making it almost impossible to sample configurations in which the longest loop is the unknotted one. Indeed, since the knot is rather localized, its freedom to place itself along the loop multiplies by a factor roughly proportional to the length of the loop itself the number of configurations accessible in its absence. By putting a  $4_1$  knot against another  $4_1$  knot, within error bars, we found the same value of  $t$  (Fig. 4). Thus, like in the previous strategy,  $t$  appears universal with respect to the prime knot type. We also carried out simulations in which one loop contained a trefoil, while the other one was tied into a composite knot made, e.g., by the product  $3_1\#3_1$  of two trefoils [26]. In this case the loop hosting the composite knot almost constantly dominates in length because both components are rather localized and free to move independently along it. In spite of the different conditions of entropic balance, we verified that also in this case the average length of the (shorter) loop with a single knot satisfies Eq.(1) with the same  $t \sim 0.75$  (Fig. 4).

The above results have implications for the leading scaling correction to the singular

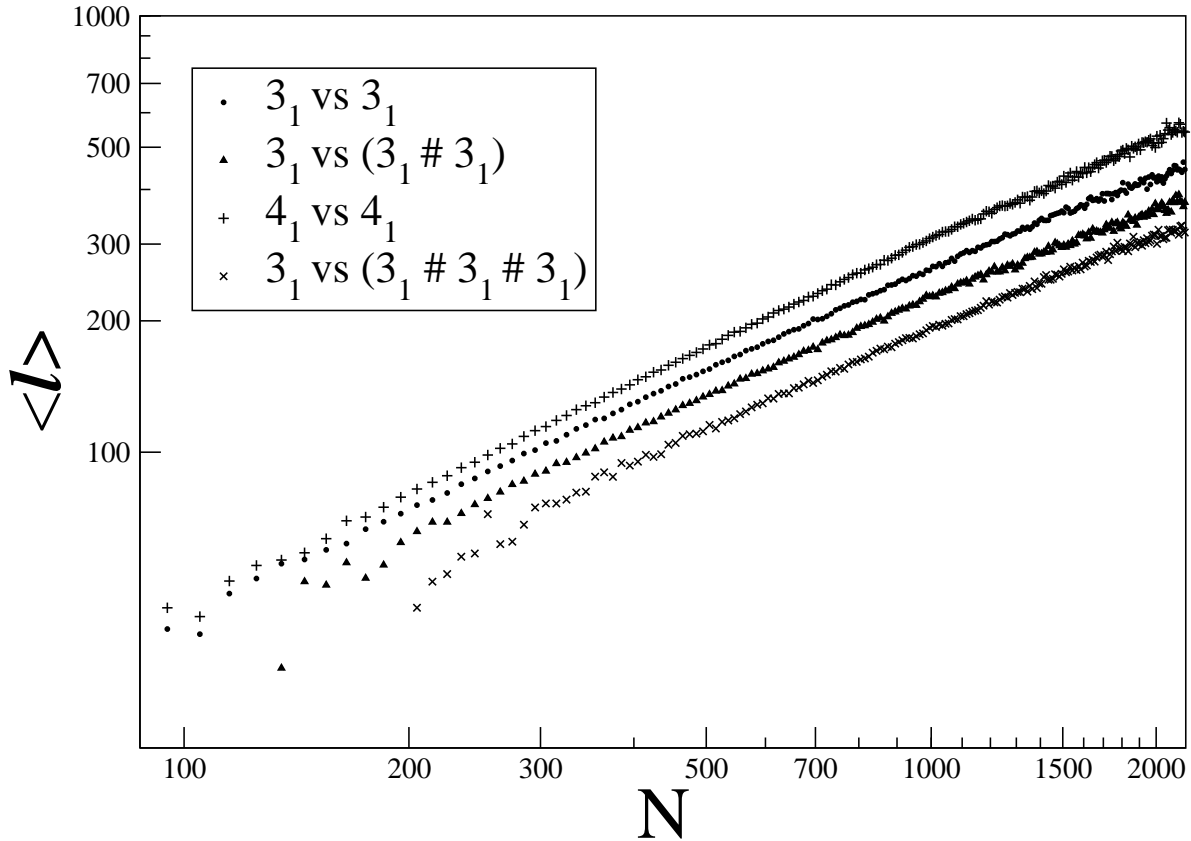


**Figure 4.** Log-log plot of the average value of the length  $l$  of the shortest loop as a function of  $N$ . Different curves correspond to the presence of different knots in the two loops. Best fit estimates of  $t$  are  $0.74 \pm 0.05$ ,  $0.75 \pm 0.03$ ,  $0.77 \pm 0.10$ ,  $0.74 \pm 0.05$  for  $3_1$  vs  $3_1$ ,  $3_1$  vs  $3_1 \# 3_1$ ,  $4_1$  vs  $4_1$  and  $3_1$  vs  $3_1 \# 3_1 \# 3_1$ , respectively.

behavior of quantities like the average radius of gyration of the SAP,  $\langle R_g^2 \rangle^{1/2} \sim AN^\nu(1 + BN^{-\Delta})$ . Field theoretical renormalization group (RG) methods [31] and most Monte Carlo techniques [32] allow to determine exponents like  $\nu \simeq 0.588$  and  $\Delta \sim 0.50$  in ensembles in which configurations with all possible ring topologies are sampled.  $\nu$  is believed to remain the same in ensembles like those considered here, with fixed knot topology [13]. With our first cutting and closing method, we could check that the ring portion occupied by the knot has an average radius of gyration  $\sim l^{\nu_0}$ , with  $\nu_0 \simeq 0.60 \simeq \nu$ . This means that a length diverging as  $\langle R_0 \rangle \sim N^{\nu t}$  exists in addition to the leading one  $\langle R_g^2 \rangle^{1/2} \sim N^\nu$ . Standard scaling arguments then lead to expect a possible strong correction exponent  $\Delta = 1 - t \sim 0.25$  for the ensemble with fixed knot topology. Such stronger correction could be quite difficult to identify numerically at relatively short  $N$  [33].

Our strategy based on entropic competition has the advantage of being applicable also to situations in which the polymer is compact. Indeed, since this method does not involve cutting and closing procedures, there is no risk that the knot topology gets altered, a highly probable event for compact configurations. This enabled us to address another key open issue in the field, namely the possible occurrence of knot delocalization

in the compact regime [18]. We included nearest neighbor attractive interactions for the two loop model and simulated it extensively at  $T \sim 0.53T_\theta$ , where  $T_\theta$  is the theta temperature [21, 25]. Below the theta point it becomes more difficult to sample long SAP configurations. Indeed, at  $T < T_\theta$ , as the critical edge fugacity is approached from below, the grand-canonical average number of SAP edges,  $\langle N \rangle_{g.c.}$ , undergoes a first order infinite jump from a finite value, rather than growing continuously to infinity as in the  $T > T_\theta$  case. In spite of this difficulty, we could get rather clear evidence that the canonical average  $\langle l \rangle$  grows linearly with  $N$  up to  $N \sim 700$ , implying  $t \simeq 1$ , for the case of two competing  $3_1$  knots (Fig. 5). Like when dealing with the good solvent regime, in order to interpret the length of the shorter loop as the knot length, it is important to check what happens to the length of a loop without knot. We got evidence that in the compact regime an unknotted loop is also delocalized, i.e. shows an average length proportional to  $N$ . However, the proportionality constant is about one order of magnitude smaller than that observed for the knotted loop in Fig. 5. Thus, knot delocalization seems to superimpose itself to a phenomenon of unknotted loop delocalization which is qualitatively similar, although quantitatively much less pronounced. The entropic competition between loops in the compact phase does not lead to a strong prominence of one of them on the other, like at high  $T$ . To the contrary, all loop length ratios are realized with comparable probability. In this new scenario also the entropic mechanisms determining knot localization in the good solvent case cease to be active.

The delocalization of prime knots in compact polymer rings opens intriguing perspectives on how topological entanglement combines with more geometrical measures of complexity in polymers. One such measure for a fluctuating SAP is the mean number of crossings,  $N_c$ , one obtains by projecting on all possible planes a given configuration [15]. This quantity can be studied also for ideal knots [10], and has been shown to be correlated with the mobility under electrophoresis of non-ideal knotted polymer rings with the same topology [34]. For ideal knots,  $N_c$  is expected to grow as  $l_{id}^{4/3}$ , where  $l_{id}$  is the length of the knot (four third power law)[11, 12]. For fluctuating, nonideal polymers one can consider the average of  $N_c$  over all configurations. It is expected that quite generally, for a compact SAP,  $\langle N_c \rangle \sim N^{4/3}$  [35]. This result should indeed hold even for open walks and be independent of topology for knotted SAP. The fact that we find  $\langle l \rangle \sim N$  for a fluctuating, knotted compact SAP suggests that for real knotted polymer rings a statistical generalization of the four third power law of ideal knots should hold:  $\langle N_c \rangle \sim \langle l \rangle^{4/3}$ . In the case of ideal knots the growth of  $l_{id}$  corresponds to an increase of the topological complexity of the knot considered [11, 12, 34]. For real knotted rings the topology remains fixed with increasing  $N$ , while fluctuations are able to produce the same type of growth of  $\langle l \rangle$  versus  $\langle N_c \rangle$ .

In conclusion, we gave a consistent and robust statistical description of the localization properties of prime knots in polymers. Weak localization and delocalization hold in the good solvent and collapsed regimes, respectively.

This work was supported by MIUR-COFIN03, FIRB01 and INFN-PAIS02.

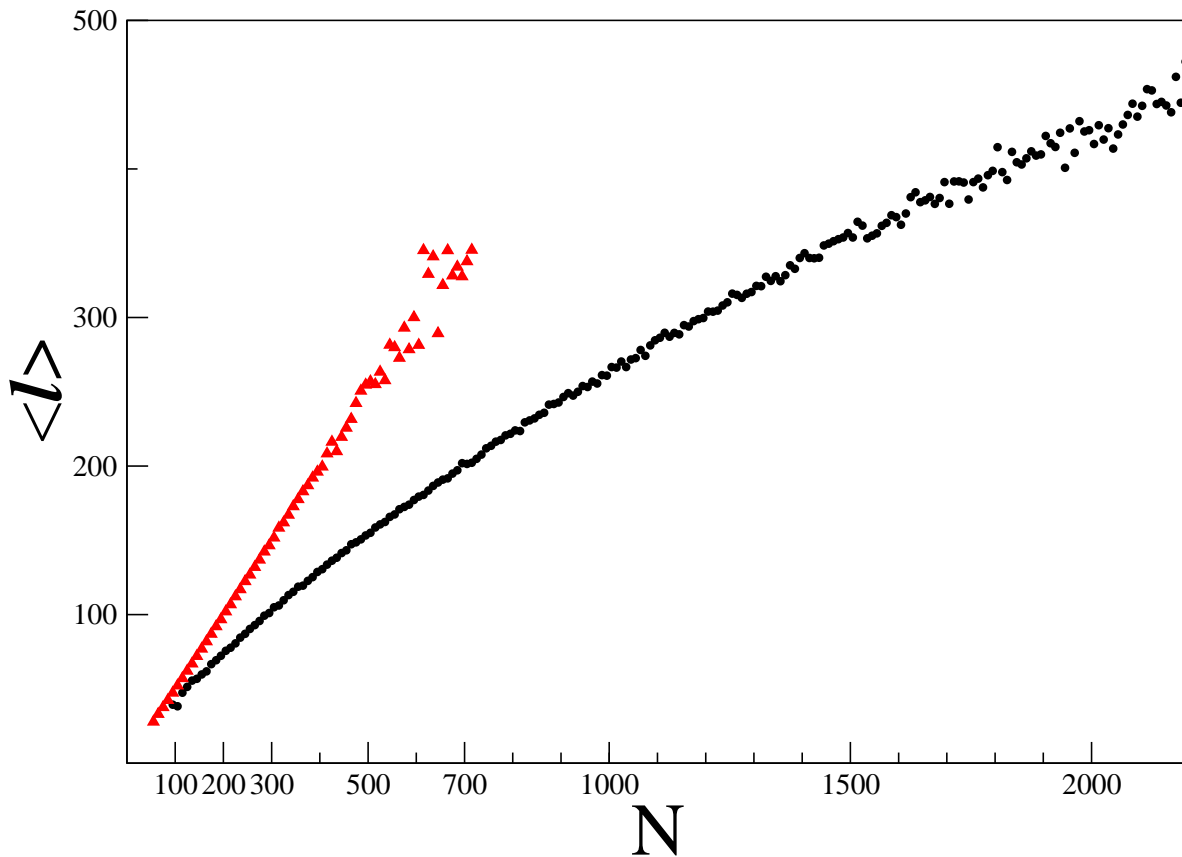


**Figure 5.** Plots of  $\langle l \rangle$  of the shortest loop as a function of  $N$ . Both curves correspond to the presence of one  $3_1$  in each loop. The bottom curve refers to  $T \gg T_\Theta$  whereas the top to  $T < T_\Theta$ .

## References

- [1] D.W. Sumners, and S.G. Whittington, *J. Phys. A: Math. Gen.* **21**, 1689 (1988).
- [2] K. Koniaris and M. Muthukumar, *Phys. Rev. Lett.* **66**, 2211 (1991).
- [3] H.L. Frisch, and E. Wasserman, *J. Am. Chem. Soc.* **83**, 3789 (1968).
- [4] S.A. Wasserman, and N.R. Cozzarelli, *Science* **232**, 951 (1986).
- [5] D.W. Sumners, *Notices of the AMS*, **42**, 528 (1995).
- [6] Y. Arai, R. Yasuda, K. Akashi, Y. Harada, H. Miyata, K. Kinoshita and H. Itoh, *Nature* **399**, 446 (1999).
- [7] X.R. Bao, H. J. Lee, and S.R. Quake, *Phys. Rev. Lett.* **91**, 265506 (2003).
- [8] J. Yan, M.O. Magnasco, and J. F. Marko, *Nature* **401**, 932 (1999).
- [9] W.R. Taylor, *Nature* **406**, 916 (2000).
- [10] V. Katrich, J. Bednar, D. Michoud, R.G. Scharein, I. Dubochet, and A. Stasiak, *Nature* **384**, 142 (1996).
- [11] J. Cantarella, D. De Turck, and H. Gluck, *Nature* **392**, 237 (1998).
- [12] G. Buck, *Nature* **392**, 238 (1998).
- [13] E. Orlandini, M.C. Tesi, E.J. Janse van Rensburg, and S.G. Whittington, *J. Phys. A: Math. Gen.* **31**, 5953 (1998).
- [14] V. Katrich, W.K. Olson, A. Vologodskii, J. Dubochet, and A. Stasiak, *Phys. Rev. E.* **61**, 5545 (2000).
- [15] E.J. Janse van Rensburg, D.W. Sumners, E. Wasserman, and S.G. Whittington, *J. Phys. A* **25**,



- 6557 (1992).
- [16] E. Gitter, and E. Orlandini, J. Phys A: Math. Gen. **32**, 1359 (1999).
  - [17] R. Metzler, A. Hanke, P.G. Dommersnes, Y. Kantor, and M. Kardar, Phys. Rev. Lett. **88**, 188101 (2002).
  - [18] E. Orlandini, A.L. Stella, and C. Vanderzande, Phys. Rev. E. **68**,031804 (2003); J. Stat. Phys. **115** , 681 (2004).
  - [19] A. Hanke, R. Metzler, P.G. Dommersnes, Y. Kantor, and M. Kardar, Eur. Phys. J. E **12**, 347 (2003).
  - [20] R. C. Lua, N. T. Moore, and A. Yu. Grosberg, cond-mat/0403413.
  - [21] C. Vanderzande, *Lattice models of Polymers*, (Cambridge University Press, Cambridge 1998)
  - [22] S. Caracciolo, A. Pellissetto and A.D. Sokal, J. Stat. Phys , 1 (1990).
  - [23] E.J. Janse van Rensburg and S.G. Whittington, J. Phys A: Math. Gen. **24**, 5553 (1991).
  - [24] C. Geyer, Computing Science and Statistics: Proceedings of the 23rd Symposium on the Interface, 156 (1991).
  - [25] M.C. Tesi, E.J. Janse van Rensburg, E. Orlandini, and S.G. Whittington J. Stat. Phys. **29**, 2451 (1996).
  - [26] D. Rolfsen, *Knots and Links*, (Berkely, CA: Publish or Perish)(1990), A. V. Vologodskii *et al.*, Sov. Phys. J.E.T.P **66**, 2153 (1974).
  - [27] In fact the Alexander polynomial is not a perfect invariant, and is unable to distinguish every knot-type. For instance the prime knot  $8_{11}$  has the same Alexander polynomial as the composite knot  $3_1\#6_1$ , and  $8_{15}$  has the same Alexander polynomial as  $3_1\#7_2$ . To distinguish pairs of knots we have also computed  $\Delta(-2)$ .
  - [28] Details will be given elsewhere.
  - [29] Similar procedures were used in Ref. [14,15] without addressing asymptotic properties like Eq. (1). For  $N = 500$  our algorithm misidentifies  $\sim 5$  out of 1000 unknotted SAP's, a much better rate than that reported in Ref. [14] for phantom rings.
  - [30] An entropic competition between independent knotted loops was recently studied in R. Zhandi, Y. Kantor, and M. Kardar, ARI, The Bulletin of the ITU, **53**, 6 (2003).
  - [31] R. Guida and J. Zinn-Justin, J. Phys. A **31**, 8103 (1998).
  - [32] B. Li, N. Madras and A.D. Sokal, J. Stat. Phys. **80**, 661 (1995).
  - [33] However, accurate studies of the effects of topological constraints on scaling, as in A. Dobay, J. Dubochet, K. Millett, P. Sottas, and A. Stasiak, Proc. Nat. Acad. Sci. **100**, 5611 (2003), should take it into account. An attempt to determine  $\Delta$  from the response of a knotted polymer to an applied force gave  $\Delta = 0.6 \pm 0.1$ , which was interpreted as implying  $t \simeq 0.4$ . See O. Farago, Y. Kantor, and M. Kardar, Europhys. Lett. **60**, 53 (2002).
  - [34] Stasiak, A., Katrich, V., Bednar, J., Michoud, D. & Dubochet, J., Nature **384**,122 (1996).
  - [35] P. Grassberger, J. Phys. A **34**, 9959 (2001).